

Search for Near-Infrared Pulsation of the Anomalous X-ray Pulsar 4U 0142+61

Mikio MORII¹, Naoto KOBAYASHI², Nobuyuki KAWAI³, Hiroshi TERADA⁴,
Yasuyuki T. TANAKA⁵, Shunji KITAMOTO¹, and Noriaki SHIBAZAKI¹

¹*Department of Physics, Rikkyo University, Nishi-ikebukuro 3-34-1,
Toshima-ku, Tokyo 171-8501, Japan
mmorii@rikkyo.ac.jp*

²*Institute of Astronomy, Graduate School of Science, University of Tokyo, 2-21-1 Osawa,
Mitaka, Tokyo 181-0015, Japan*

³*Department of Physics, Tokyo Institute of Technology, Ookayama 2-12-1, Meguro-ku,
Tokyo 152-8551, Japan*

⁴*Department of Earth and Planetary Science, University of Tokyo, 7-3-1 Hongo, Bunkyo-ku,
Tokyo 113-0033, Japan*

⁵*Subaru Telescope, National Astronomical Observatory of Japan, 650 North A'ohoku Place,
Hilo, HI 96720, USA*

(Received 2008 June 16; accepted 2008 September 9)

Abstract

We have searched for pulsation of the anomalous X-ray pulsar (AXP) 4U 0142+61 in the K' band ($\lambda_{\text{eff}} = 2.11 \mu\text{m}$) using the fast-readout mode of IRCS at the Subaru 8.2-m telescope. We found no significant signal at the pulse frequency expected by the precise ephemeris obtained by the X-ray monitoring observation with RXTE. Nonetheless, we obtained a best upper limit of 17% (90% C.L.) for the root-mean-square pulse fraction in the K' band. Combined with i' band pulsation (Dhillon et al. 2005), the slope of the pulsed component ($F_\nu \propto \nu^\alpha$) was constrained to $\alpha > -0.87$ (90% C.L.) for an interstellar extinction of $A_V = 3.5$.

Key words: stars: neutron — stars: pulsars: individual (4U 0142+61)

1. Introduction

Anomalous X-ray pulsars (AXPs; see Woods, & Thompson (2006) for a recent review) have been recognized as being enigmatic X-ray pulsars, for which none of characteristics of binary companions have been detected (Mereghetti & Stella 1995). Therefore, the observed X-ray luminosity of AXPs ($L_X \sim 10^{34} - 10^{36} \text{ erg s}^{-1}$) cannot be explained by the accretion of

matter from companions, as is the case for binary X-ray pulsars. The spin periods of AXPs (P) are concentrated in a narrow range ($2-12$ s¹) and the spin-down rates (\dot{P}) are distributed in the range $5 \times 10^{-13} - 1 \times 10^{-10}$ s s⁻¹. The rate of the spin-down energy loss of neutron stars ($\dot{E} = -4\pi^2 I \dot{P} / P^3 \sim 10^{32.6}$ erg s⁻¹, where $I \simeq 10^{45}$ g cm² is the moment of inertia of a neutron star) is too small to maintain the X-ray luminosity, suggesting that they are not rotation-powered pulsars.

Two competing models have been proposed for the energy source: accretion from a fossil disk and decay of ultra-strong magnetic fields. In the former scenario, the fossil disks are thought to be produced through a fall-back of matter after a supernova explosion (Chatterjee, Hernquist & Narayan 2000; Chatterjee & Hernquist 2000; Alpar 2001) or as a remnant of the common-envelope phase in the evolution of a binary (van Paradijs, Taam & van den Heuvel 1995; Ghosh, Angelini, & White 1997). The advantage of the fossil disk model is that it naturally explains the narrow range of the concentration of the spin periods through the propeller phase in the spin evolution (Chatterjee, Hernquist & Narayan 2000; Chatterjee & Hernquist 2000; Alpar 2001). In the latter scenario AXPs are magnetars, which are strongly magnetized neutron stars with emissions powered by the dissipation of magnetic energy (Thompson & Duncan 1995; Thompson & Duncan 1996). Assuming that their spins are braked by magnetic dipole radiation, a strong magnetic field of $10^{14} - 10^{15}$ G at their surface is implied. AXPs are similar to soft gamma repeaters (SGRs), which are thought to be magnetars (e.g. see Thompson & Duncan 1995). The observation of SGR-like bursts in AXPs suggests the unification of AXPs and SGRs by the magnetar scenario (Gavriil, Kaspi, & Woods 2002).

4U 0142+61 is a typical object among AXPs. It is the nearest and least absorbed object among AXPs and SGRs and is hence the most intensively observed of these objects in multi-wavelength studies. The optical counterpart of this object was discovered by Hulleman, van Kerkwijk & Kulkarni (2000). Kern & Martin (2002) discovered the optical pulsation. The pulsed fraction of $PF_{\text{opt}} = 27_{-6}^{+8}\%$ was found to be larger than that of soft X-rays, suggesting that the optical pulsation cannot be explained by thermal reprocessing of a disk illuminated by X-rays. Dhillon et al. (2005) also measured the optical pulsation in a i' band and obtained a consistent pulsed fraction of $PF_{i'} = 29 \pm 8\%$.

We showed that the near-infrared/optical spectrum consists of two components, near-infrared excess and optical pulsating components, by first near-simultaneous multi-band photometry (Morii et al. 2005; Tanaka et al. 2008). Wang, Chakrabarty & Kaplan (2006) discovered the mid-infrared emission with Spitzer, and showed that the near-infrared excess component extends to the mid-infrared region. They proposed that the infrared excess component can be modeled by a dust disk around a neutron star, where the spectrum is similar to that of the dust disk of a proto-planetary system. Their model is different from the original fossil disk

¹ Recently, the period range was extended down to 2 s by the discovery of the radio-emitting AXP 1E 1547.0–5408 (Camilo et al. 2007).

model, in that the disk does not power the X-ray emission. In their model, the flux of the K band is mainly composed of the dust disk component. Therefore, the pulsed flux of the K band is expected to be small. Durant & van Kerkwijk (2006b) collected data spanning seven years and showed that the near-infrared/optical flux and the spectral shape are variable. The correlations between the X-ray total/pulsed fluxes and the near-infrared/optical fluxes were uncertain, although these correlations are expected for a fossil disk. Therefore, they suggested that the near-infrared flux is composed of components other than the disk component. As described above, the origin of the infrared emission is not yet clear.

Some authors have proposed theoretical models for the optical/infrared emission of AXPs, based on the magnetar scenario or fossil disk scenario. In the former scenario, Eichler, Gedalin & Lyubarsky (2002); Lu & Zhang (2004) applied mechanisms of coherent radio emission of rotation-powered pulsars to a magnetar, where the emission frequency is boosted to the infrared, optical, or even UV region by the strong magnetic field of the magnetar. Heyl & Hernquist (2005) proposed an exotic quantum electrodynamics model for the broad-band emission of magnetars. Ertan & Cheng (2004) applied the outer gap model of rotation-powered gamma-ray pulsars on magnetars. In the latter scenario, Perna, Hernquist & Narayan (2000); Perna & Hernquist (2000); Hulleman, van Kerkwijk & Kulkarni (2000) discussed the optical/infrared spectrum generated by an irradiated fall-back disk and found that the sizes of the inner and outer radii of the disk become implausible. In addition, hybrid models of both scenarios have also been proposed. Ertan & Cheng (2004) showed that the pulsed optical emission can be explained by the disk-star dynamo gap model, where the fossil disk plays a key role in the emission mechanism. Ertan & Çalişkan (2006); Ertan et al. (2007) showed that an irradiated and viscously heated disk model can account for the observed infrared/optical spectrum of both pulsed and un-pulsed components, by magnetospheric optical emission (Ertan & Cheng 2004) and disk emission, respectively.

In any of the above models, the origin of the emission can be clearly determined by the pulsation. The emission from the co-rotating magnetosphere must be pulsed, while that from the disk is unlikely to be pulsed. In this paper, we report a search for the pulsation of the AXP 4U 0142+61 in the K' band, using the fast-readout mode of IRCS mounted on the Subaru 8.2-m telescope. This is the first search for the pulsation in the infrared band.

In the following, the dereddened spectrum of 4U 0142+61 is obtained using the interstellar extinction of $A_V = 3.5 \pm 0.4$, which was determined by using red clump stars (Durant & van Kerkwijk 2006a).

2. Observation

We observed the AXP 4U 0142+61 in the K' band (MKO-NIR photometric system; Simons & Tokunaga 2002) on 2004 July 31 (UT), using IRCS (Infrared Camera and Spectrograph)(Kobayashi et al. 2000; Tokunaga et al. 1998) mounted on the Cassegrain focus

Table 1. Summary of our observation

| | |
|-----------------|--|
| Date (UT) | 2004-07-31 |
| Start time (UT) | 12:57:14 |
| End time (UT) | 15:21:07 |
| Duration | 8633 s |
| Filter | K' ($\lambda_{\text{eff}} : 2.11 \mu\text{m}$) |
| NDR | 16 |
| Co-adds | 1 |
| Exposure | 0.84 s |
| # of frames | $300 \times 22 = 6600$ |
| Net exposure | 5.5 ks |
| Seeing (FWHM) | $0.''37$ |

of the Subaru Telescope (Iye et al. 2004) on top of Mauna Kea, Hawaii. The weather condition was photometric with an excellent seeing ($\sim 0.''4$ at the K' band) through the observing. In the MKO-NIR photometric system, the effective wavelength and band width of the K' band are $\lambda_{\text{eff}} = 2.11 \mu\text{m}$ and $\Delta\lambda = 0.34 \mu\text{m}$ (FWHM), respectively (Tokunaga, Simons & Vacca 2002; Tokunaga & Vacca 2005). To search for pulsation of the AXP, we used IRCS in the *movie mode*.

In this mode, we successively took 0.84-s exposure frames, corresponding to about 1/10 of the pulse period of the AXP (8.7 s). To reduce the overhead time for array readout and data recording, we restricted the readout region to the central sub-array of 256×256 pixels, which corresponds to 1/8 of the 1024×1024 pixels of the full image. We used a pixel scale of 58 mas per pixel, and hence the 256×256 -pixel region corresponded to a field of view (FoV) of $14''.8 \times 14''.8$.

We observed the AXP by two-point dithering. We arranged the FoV of IRCS so that at least one of two bright stars near the AXP (109 and 115 listed in Hulleman, van Kerkwijk & Kulkarni 2004) were included in the FoVs of both observation directions. We call one of the two directions, for which star 109 and the AXP were included in the FoV, the “A direction,” and we call the other, for which stars 115 and 109 and the AXP were included in the FoV, the “B direction.” These stars were bright enough to be seen in all frames. We successively took 300 frames for each direction, saved into a FITS file of cube structure, called a “data-cube”, and recorded the instantaneous time of each frame. The observation directions were changed in the order A, A, B, B, A, A, Good quality data taken in our observation are summarized in table 1.

3. Analysis

3.1. Search for Pulsation

The precise pulse frequency of 4U 0142+61 has been measured with RXTE over a period of ten years (Dib, Kaspi & Gavriil 2007). The period of our Subaru observation is included in this interval. The pulse frequency of this AXP at the start of our Subaru observation was 0.1150934471(15) Hz, where the number in parentheses is the 1σ uncertainty. Here, we used the “Postgap ephemeris spanning cycle 5–10” in table 2 of Dib, Kaspi & Gavriil (2007).

We searched for pulsation in our Subaru data near this pulse frequency by the epoch folding method from 0.113601 Hz to 0.116601 Hz in steps of 0.00001 Hz. The range and step were sufficiently wide and fine, respectively, because the Fourier resolution of the pulse frequency was $\Delta\nu = 1/2T = 5.8 \times 10^{-5}$ Hz, where T is the observation span (table 1). Since the pulse period of the AXP is long (8.7 s) and the duration of the observation was short (2.4 hours), the only significant effect of the Doppler shift due to the motion of observer was that due to the orbital motion of the earth, estimated to be $\Delta\nu = +7.6 \times 10^{-6}$ Hz. This is small in comparison with the Fourier resolution. Thus, barycentric correction of the arrival times of photons was not necessary in our observation.

We analysed the data with the IRAF software packages. We decomposed the data-cubes of the A and B directions into normal FITS images, A_i and B_i ($i = 1, 2, \dots, 300$). The first image of each data-cube was excluded, because its quality was poor owing to bias instability. We produced $A_i - B_i$ images ($i = 2, 3, \dots, 300$), by subtracting a frame of the B direction from a frame of the A direction. By this process, the sky background and the dark level were canceled. The pair of data-cubes were selected with as small an interval between the directions as possible to cancel the sky background properly. Subtraction between frames of the same index i was necessary to cancel the sequencing variation of the bias. $B_i - A_i$ images were also produced in the same way. Flat fielding was performed for the $A_i - B_i$ and $B_i - A_i$ images using a mean-combined flat frame taken by irradiation of a calibration lamp.

We sorted the flat-fielded images into eight phases of a tentative pulse period of the AXP, according to the instantaneous times at their exposures. For each phase, we shifted and combined the flat-fielded images by masking the bad pixels. The map of the bad pixels was made from the dark and flat frames, for which we selected pixels with extraordinary ADU counts. The number of pixels for the image-shift was calculated by measuring the center position of the point spread function of the two bright stars (109 and 115; see section 2).

We measured the flux (ADU) of the AXP of each phase using the standard IRAF photometry package (PHOT). For the aperture, we set the radii from 1 pixel ($0''.058$) to 15 pixels ($0''.87$) in steps of 1 pixel. For the background region, we set a concentric annulus with radii of the inner and outer boundaries of 15 and 25 pixels ($1''.45$). The systematic error of the flux was estimated by photometry for 11 areas of blank sky for the same aperture and background

annulus as the area of the AXP. In the following, we applied an aperture radius of 4 pixels (0."23). For an aperture radius of around 4 pixels, the signal-to-noise ratio of the flux within the aperture to the systematic error obtained as above became maximum for a phase-averaged image (figure 1). We produced a pulse profile with eight phase bins, and calculated the reduced χ^2 values for the profile by the best fit constant model. The reduced χ^2 value represents the signal of the pulsation of the AXP. Figure 2 shows the signal versus the pulse frequency. We could not detect any significant signal of pulsation of the AXP at the expected pulse frequency in any aperture radius setting.

In addition, we tried a similar pulse search by relative photometry with reference to the flux of stars 109 or 106 listed in Hulleman, van Kerkwijk & Kulkarni (2004) (figure 1). For star 109, the values in a plot corresponding to figure 2 was larger than that obtained by the simple photometry above. It is thought that there is an adverse influence of the dimple of star 115 close to star 109. In contrast, for star 106 the reduced χ^2 values were slightly smaller, indicating a slight improvement of the photometry. Since this improvement was small, we decided to apply simple photometry rather than relative photometry with reference to star 106.

3.2. Upper Limit for Pulsation

The infrared pulse profile of 4U 0142+61 is unknown. Then, at first we calculated an upper limit of the pulse fraction by the root-mean-square pulse fraction (van der Klis 1989):

$$PF_{\text{rms}} = \frac{\sqrt{\frac{1}{N} \sum_i (R_i - \bar{R})^2}}{\bar{R}},$$

where R_i ($i = 1, 2, \dots, N; N = 8$) and \bar{R} are the flux of 4U 0142+61 of the i -th phase bin and the mean of R_i , respectively. We produced a histogram of PF_{rms} of a pulse profile for the searched pulse frequencies, and hence the 90% C.L. upper limit was obtained from the distribution of the histogram. We followed this calculation for each aperture radius, and the least upper limit was obtained at an aperture radius of 5 pixels (0."29). The 90% C.L. upper limit of the pulse fraction was 17%.

Assuming the pulse profile, the tighter upper limit can be obtained. Because of the non-detection of the infrared pulsation, an assumption of a sinusoidal shape is generally acceptable. For 4U 0142+61, both single-peaked and double-peaked shapes are plausible. For example, the optical pulse profile shown in Kern & Martin (2002) is a double-peaked shape, while that shown in Dhillon et al. (2005) looks like a single-peaked shape. Then, we fitted the pulse profile by a sine curve with three free parameters (PF_{sin} , B and δ),

$$F = B \times [PF_{\text{sin}} \sin(2\pi\phi + \delta) + 1]$$

or

$$F = B \times [PF_{\text{sin}} \sin(4\pi\phi + \delta) + 1]$$

with the χ^2 fitting method for each pulse frequency and each aperture radius. Here, ϕ is the

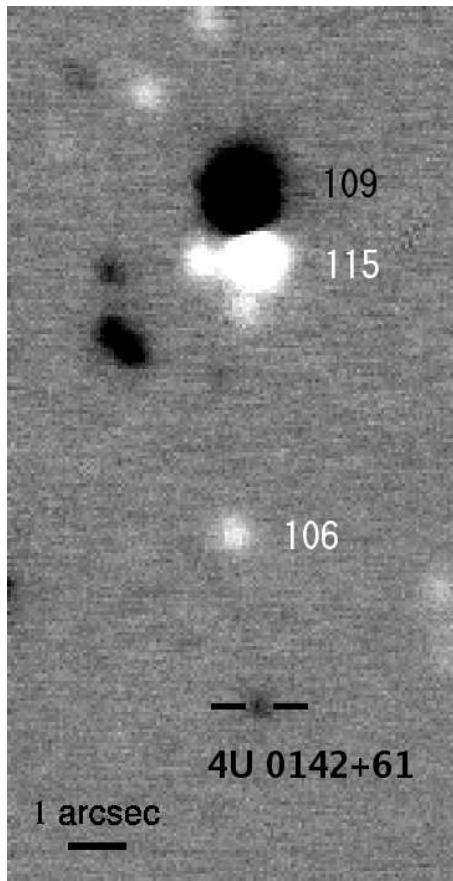


Fig. 1. K' image of the field around 4U 0142+61, generated by combining all the images of the IRCS movie mode. A $1''$ scale is shown in the bottom-left corner of the image. 4U 0142+61 is indicated by two horizontal bars with a spacing of 8 pixels ($0.''46$). The brightest star in the upper region is star 109 (see section 2). The dimples of inverted color are side-effects of the generation of the $A_i - B_i$ and $B_i - A_i$ images. For example, dimples corresponding to stars 115 and 106 were appeared by processes $A_i - B_i$ and $B_i - A_i$, respectively.

pulse phase between 0 and 1. We followed the same method as that described in PF_{rms} for the calculation of the 90% C.L. upper limit of the PF_{sin} . The least 90% C.L. upper limit of the pulse fraction was both 16% at aperture radii of 5 pixels and 3 pixels ($0.''17$), respectively.

Eventually, the resultant upper limit of the pulse fraction is 17% (90% C.L.) by selecting a conservative value.

3.3. Phase-averaged flux

The phase-averaged flux of 4U 0142+61 was obtained by relative photometry of an image made by combining all the images of the movie mode (figure 1). The magnitude of the AXP was measured with reference to the magnitude of star 106 listed in Hulleman, van Kerkwijk & Kulkarni (2004). The aperture radius and the radii of the inner and outer boundaries of the concentric annulus for the background were set to 4, 15 and 25 pixels, respectively.

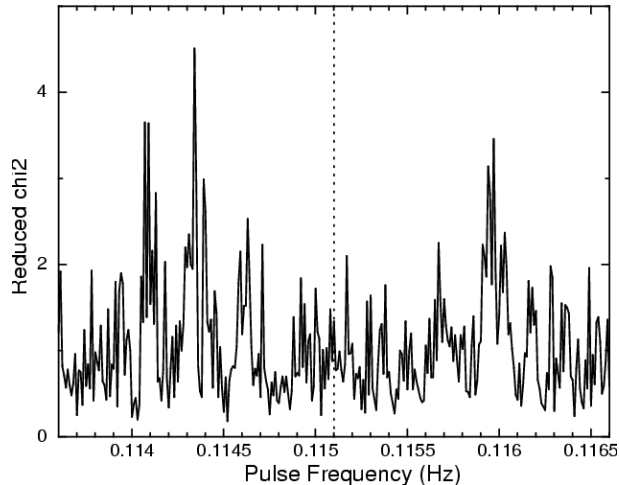


Fig. 2. Result of pulse search for an aperture radius of 4 pixels ($0.''23$). The vertical dotted line denotes the expected pulse frequency (see text).

The systematic error for the flux was estimated as described in subsection 3.1. The resultant magnitude of the AXP was $K' = 19.73 \pm 0.09 \pm 0.03$, where the last error is the zero-point uncertainty inherited from the catalog (Hulleman, van Kerkwijk & Kulkarni 2004).

4. Discussion

To discuss the emission mechanism of the AXP, we generated the spectral energy distribution (νF_ν) of 4U 0142+61 for the phase-averaged fluxes and pulsed fluxes (figure 3), using all the published data (see caption of figure 3) and the K' band fluxes obtained in this work.

For the Subaru observation on Sep. 2003 (Morii et al. 2005), we analysed the data in our own way and obtained different results from that shown in Durant & van Kerkwijk (2006b). We will present the details of the photometry in our companion paper (Tanaka et al. 2008). In the phase-averaged spectrum, a peak at the H band is clearly seen. As discussed in Hulleman, van Kerkwijk & Kulkarni (2004), this feature may be a proton cyclotron feature. Although other cyclotron features in other bands are expected, they are not yet clear. Further simultaneous multi-band observations are necessary, because the spectrum is variable.

To understand the emission mechanism of the pulse component, we calculated the slope of the spectral shape. Combined with the pulsed flux of the K' band (this work; PF_{rms}) and that of the i' band (Dhillon et al. 2005), the slope of the pulsed component ($F_\nu \propto \nu^\alpha$) was found to be constrained to $\alpha > -0.87$ (90% C.L.) for the interstellar extinction of $A_V = 3.5$.

Because the constraint on the slope of the pulsed flux is not so stringent, any emission mechanisms are still allowed for the pulse component. For example, the Rayleigh-Jeans tail of the blackbody is $\alpha = +2$ and synchrotron self-absorption is $\alpha = +2.5$. In the quantum electrodynamics model of Heyl & Hernquist (2005), $\alpha = 0$ for the optical-infrared region. In the disk-star dynamo gap model of Ertan & Cheng (2004), $\alpha = -0.5$; while in the magnetar

model by the same authors, α is slightly smaller than -0.5 .

In the curvature-drift-induced maser mechanism proposed by Lu & Zhang (2004), the maser frequency of 4U 0142+61 is about $\nu_M = 1.39 \times 10^{14}$ Hz, which is near the K band. Then, the maser amplification ratio equating to the pulse fraction in their model is maximum near the K band. Since the upper limit for the pulse fraction of the K' band is similar to the pulse fraction of the i' band, this model is a possible mechanism. The H band peak in the phase-averaged spectrum may be the maser frequency peak of this emission mechanism. If so, then a larger pulse fraction at the H band is expected.

Viewed differently, the dust disk model is also a possible mechanism (Wang, Chakrabarty & Kaplan 2006), because the fraction of un-pulsed flux is dominant in the K' band.

In the near future, we can make use of the adaptive optics (AO) technique for the sensitive detection of the AXP. The Subaru Telescope plans to install an upgraded 188-element AO system with a laser guide star (Hayano et al. 2003). Using this technique, we will be able to constrain the pulse fraction to $PF < 3\%$ and constrain the spectral slope of the pulsed component to $\alpha > 1$ for a feasible observation time. Furthermore, the K band flux varies about 40% over the time scale of years and hence it is possible that the K band pulsation would grow above the detection limit. Further monitoring of the infrared pulsation should prove interesting.

M. M. is supported by the Post-doctoral Researchers Program of Rikkyo University and a Grant-in-Aid for Young Scientists(B)(18740120).

References

- Alpar, M. A. 2001, ApJ, 554, 1245
Camilo, F., Ransom, S. M., Halpern, J. P. & Reynolds, J. ApJ, 666, L93
Chatterjee, P., Hernquist, L. & Narayan, R. 2000, ApJ, 534, 373
Chatterjee, P. & Hernquist, L. 2000, ApJ, 543, 368
Chiar, J. E. & Tielens, A. G. G. M. 2006, ApJ, 637, 774
Dib, R., Kaspi, V. M. & Gavriil, F. P. 2007, ApJ, 666, 1152
Dhillon, V. S., Marsh, T. R., Hulleman, F., van Kerkwijk, M. H., Shearer, A., Littlefair, S. P., Gavriil, F. P., & Kaspi, V. M. 2005, MNRAS, 363, 609
Durant, M & van Kerkwijk, M. H. 2006a, ApJ, 650, 1070
Durant, M & van Kerkwijk, M. H. 2006b, ApJ, 652, 576
Eichler, D., Gedalin, M. & Lyubarsky, Y. 2002, ApJ, 578, L121
Ertan, Ü & Cheng, K. S. 2004, ApJ, 605, 840
Ertan, Ü & Çalişkan, Ş. 2006, ApJ, 649, L87
Ertan, Ü, Erkut, M. H., Ekşi, K. Y. & Alpar, M. A. 2007, ApJ, 657, 441
Fukugita, M., Shimasaku, K. & Ichikawa, T. 1995, PASP, 107, 945
Gavriil, F. P., Kaspi, V. M. & Woods, P. M. 2002, Nature, 419, 142
Ghosh, P., Angelini, L. & White, N. E. 1997, ApJ, 478, 713

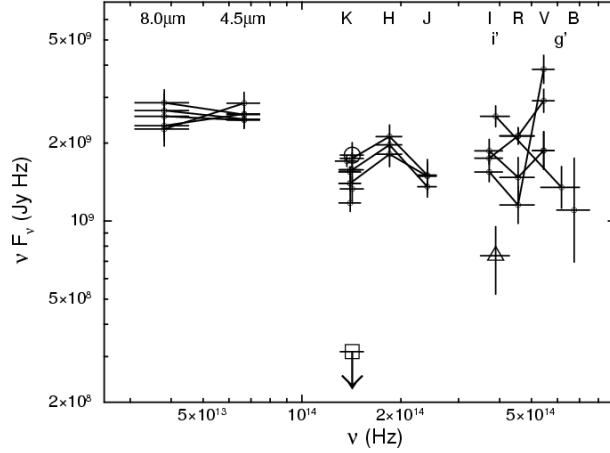


Fig. 3. Energy spectrum (νF_ν) of 4U 0142+61. The horizontal and vertical axes are shown in units of Hz and Jy·Hz, respectively. Phase-averaged fluxes derived from Hulleman, van Kerkwijk & Kulkarni (2000); Hulleman, van Kerkwijk & Kulkarni (2004); Morii et al. (2005); Durant & van Kerkwijk (2006b); Wang, Chakrabarty & Kaplan (2006); Wang & Kaspi (2008); Tanaka et al. (2008) are marked as small circles. The flux obtained by this work (see subsection 3.3) is marked as a large circle. The pulsed flux in the i' band is derived from Dhillon et al. (2005) and marked as a large triangle. The 90% C.L. upper limit for the pulsed flux in the K' band obtained in this work (PF_{rms}) is marked as a large square and downward arrow. The pulsed fluxes are calculated as the product of the phase-averaged flux and the pulse fraction. The vertical bars show the 1σ level error range. Fluxes obtained on the same day are connected by solid lines. For the Subaru Telescope data, we used the results of Morii et al. (2005) and Tanaka et al. (2008). To convert the magnitudes to fluxes, we used the zero fluxes of the Johnson-Cousins photometric system for the $IRVB$ bands of the KeckI(II)/LRIS, KeckII/ESI and UH88/Optic data, the Ellis system for the R_E band of the KeckII/ESI data, the SDSS system for the $i'g'$ bands of the UHT/ULTRACAM data (Fukugita, Shimasaku & Ichikawa 1995) and the MKO-NIR system for the $KK'Ks$ bands of the KeckI/NIRC, CFHT/AOB, Subaru/IRCS and Gemini/NIRI data (Tokunaga & Vacca 2005). We corrected the observed flux by the interstellar extinction of $A_V = 3.5$ (Durant & van Kerkwijk 2006a). Extinction other than that of the V band was calculated by the relative extinction listed in Schlegel, Finkbeiner & Davis (1998) and the extinction law given in Chiar & Tielens (2006). The systems or bands not listed in Schlegel, Finkbeiner & Davis (1998) were corrected using values of the Landolt and UKIRT systems for optical and near-infrared bands, respectively.

- Kern, B. & Martin, C. 2002, *Nature*, 417, 527
- Kobayashi, N., Tokunaga, A. T., Terada, H., Goto, M., Weber, M., Potter, R., Onaka, P. M., Ching, G. K., Young, T. T., Fletcher, K., Neil, D., Robertson, L., Cook, D., Imanishi, M. & Warren, D. W. 2000, *Proc. SPIE*, 4008, 1056
- Hayano, Y., Takami, H., Gaessler, W., Takato, N., Goto, M., Kamata, Y., Minowa, Y., Kobayashi, N. & Iye, M. 2003, *Proc. SPIE*, 4839, 32
- Heyl, J. S & Hernquist, L. 2005, *MNRAS*, 362, 777
- Hulleman, F., van Kerkwijk, M. H. & Kulkarni, S. R. 2000, *Nature*, 408, 689
- Hulleman, F., van Kerkwijk, M. H. & Kulkarni, S. R. 2004, *A&A*, 416, 1037
- Iye, M. et al. 2004, *PASJ*, 56, 381
- Lu, Y. & Zhang, S. N. 2004, *MNRAS*, 354, 1201
- Mereghetti, S. & Stella, L. 1995, *ApJ*, 442, L17
- Morii, M., Kawai, N., Kataoka, J., Yatsu, Y., Kobayashi, N., & Terada, H. 2005, *Advances in Space Research*, 35, 1177
- Perna, R., Hernquist, L. & Narayan, R. 2000, *ApJ*, 541, 344
- Perna, R. & Hernquist, L. 2000, *ApJ*, 544, L57
- Schlegel, D. J., Finkbeiner, D. P. & Davis, M. 1998, *ApJ*, 500, 525
- Simons, D. A. & Tokunaga, A. T. 2002, *PASP*, 114, 169
- Tanaka, Y. T., Morii, M., Kobayashi, N., Kawai, N., Kataoka, J., Yatsu, Y., Terada, H., Nagasaki, K., Kitamoto, S. & Shibasaki, N. 2008, in prep.
- Thompson, C. & Duncan, R. C. 1995, *MNRAS*, 275, 255
- Thompson, C. & Duncan, R. C. 1996, *ApJ*, 473, 322
- Tokunaga, A. T., Kobayashi, N., Bell, J., Ching, G. K., Hodapp, K-W, Hora, J. L., Neill, Doug, Onaka, P. M., Rayner, J. T., Robertson, L., Warren, D. W., Weber, M. & Young, T. T. 1998, *Proc. SPIE*, 3354, 512
- Tokunaga, A. T., Simons, D. A. & Vacca, W. D. 2002, *PASP*, 114, 180
- Tokunaga, A. T. & Vacca, W. D. 2005, *PASP*, 117, 421
- van der Klis, M. 1989, in “Timing Neutron Stars,” eds. Ögelman, H. and van den Heuvel, E. P. J., NATO ASI Series C, Vol. 262, p27-69, Kluwer.
- van Paradijs, J., Taam, R. E. & van den Heuvel, E. P. J. 1995, *A&A*, 299, L41
- Wang, Z. & Kaspi, V. M. 2008, *ApJ*, 675, 695
- Wang, Z., Chakrabarty, D., & Kaplan, D. L. 2006, *Nature*, 440, 772
- Woods P. M., & Thompson, C. 2006, in “Compact Stellar X-ray Sources,” eds. W. H. G. Lewin and M. van der Klis (Cambridge: Cambridge Univ. Press) (astro-ph/0406133)